ELSEVIER

Journal of Hazardous Materials B137 (2006) 344–351

Journal of Hazardous Materials

www.elsevier.com/locate/jhazmat

Kinetic and equilibrium studies on the removal of acid dyes from aqueous solutions by adsorption onto activated carbon cloth

Numan Hoda, Edip Bayram, Erol Ayranci *

Chemistry Department, Akdeniz University, Antalya 07058, Turkey

Received 14 September 2005; received in revised form 10 February 2006; accepted 10 February 2006
Available online 23 March 2006

Abstract

Removal of acid dyes Acid Blue 45, Acid Blue 92, Acid Blue 120 and Acid Blue 129 from aqueous solutions by adsorption onto high area activated carbon cloth (ACC) was investigated. Kinetics of adsorption was followed by in situ UV-spectroscopy and the data were treated according to pseudo-first-order, pseudo-second-order and intraparticle diffusion models. It was found that the adsorption process of these dyes onto ACC follows the pseudo-second-order model. Adsorption isotherms were derived at 25 °C on the basis of batch analysis. Isotherm data were treated according to Langmuir and Freundlich models. The fits of experimental data to these equations were examined.

Keywords: Acid dyes; Adsorption kinetics; Adsorption isotherm; Activated carbon cloth; Water treatment

1. Introduction

Dyes are used for coloring purposes in textile, food, paper, carpet, rubber, cosmetic and plastic industries. Synthetic dyes are produced annually over 7×10^5 t worldwide and during the coloring processes approximately 10–15% of them are lost to waste streams as pollutants [1]. Some of these dyes are toxic and suspected to have carcinogenic and mutagenic effects [2], some present an aesthetic problem and affect the nature of water reducing photosynthetic activity by inhibiting sunlight penetration [3]. Removal of synthetic dyes from wastewater before discharging to environment and from raw water before offering it to public use is essential for the protection of health and environment. Some of the techniques used in treatment of wastewaters containing dyes are flocculation, coagulation, precipitation, adsorption, membrane filtration, electrochemical techniques, ozonation and fungal decolorization [4]. Among these techniques adsorption has been shown to be an effective technique with its efficiency, capacity and applicability on a large scale to remove dyes as well as having the potential for regeneration, recovery and recycling of adsorbents [3–6]. Activated carbon, which is the most common adsorbent in liquid-phase dye adsorption process [3,7–10], can be used in granular, powder and fiber or cloth forms. In the last decade, activated carbon cloth (ACC) has appeared to be an attractive adsorbent because of its high surface area, high adsorption capacity and mechanical strength. The potential efficiency of activated carbon cloth or fiber for the removal of many pollutants from waste water by adsorption has been investigated by many workers [11–17].

The aim of the present work is to investigate the removal of some acid dyes; Acid Blue 45, Acid Blue 92, Acid Blue 120 and Acid Blue 129, from aqueous solutions by adsorption onto ACC and to determine the adsorption characteristics of ACC toward these dyes by conducting equilibrium and kinetic studies.

2. Materials and methods

2.1. Materials

ACC used in the present work was provided by Spectra Corp. (MA, USA) coded as Spectracarb 2225. The dyes; acid blue 45 (AB45), acid blue 92 (AB92), acid blue 120 (AB120) and acid blue 129 (AB129) having dye contents of 50%, 40%, 40% and 25%, respectively, were obtained from Sigma. The chemical structures of these dyes are given in Fig. 1. Deionized water was used in adsorption experiments.

* Corresponding author. Tel.: +90 242 310 23 15; fax: +90 242 227 89 11.
E-mail address: eayranci@akdeniz.edu.tr (E. Ayranci).

0304-3894/$ – see front matter © 2006 Elsevier B.V. All rights reserved.
doi:10.1016/j.jhazmat.2006.02.009

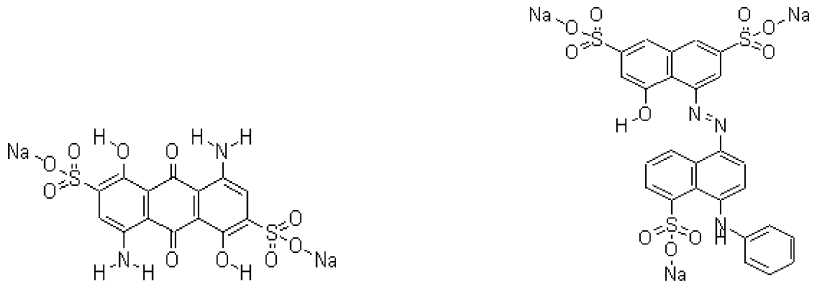

Acid Blue 45 Acid Blue 92

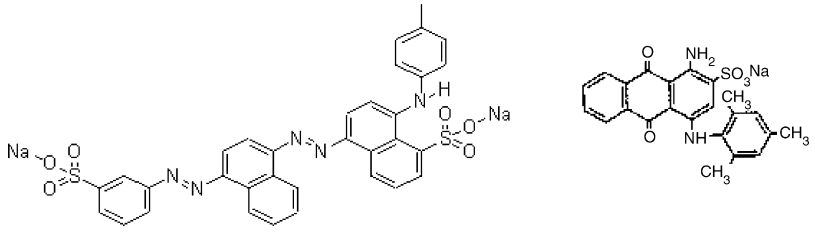

Acid Blue 120 Acid Blue 129

Fig. 1. Molecular structures of acid dyes studied.

2.2. Treatment of ACC

It was found by Ayranci and Conway [12] that ACC material provides spontaneously a small but significant quantity of ions into the conductivity water, probably due to its complex structure originating from its somewhat unknown proprietary preparation procedure. A deionization cleaning procedure was therefore applied, as described previously [12,14] to avoid desorption of ions during the adsorption measurements. In this procedure, ACC sample was placed in a flow-through washing cup and eluted with 5 L of warm (60 °C) conductivity water in a kind of successive batch operations for 2 days with N_2 bubbling in order to avoid possible adsorption of CO_2 that might have been dissolved in water. The out-flow water from each batch was tested conductometrically for completeness of the washing procedure. The washed ACC modules were then dried under vacuum at 120 °C, cut to desired dimensions (about 1.0 cm × 1.5 cm), weighed accurately and kept in a desiccator for further use.

2.3. Characterization of ACC

Prior to nitrogen adsorption experiment to determine surface properties, ACC sample was degassed at 130 °C under vacuum (up to 10^{-6} Torr) for 12 h. The N_2 adsorption data were obtained at the Central Laboratory of Middle East Technical University (METU) with a Quantachrome Autosorb-1-C/MS apparatus over a relative pressure ranging from 10^{-6} to 1. The BET specific surface area (S_{BET}), total pore volume (V_{tot}), micropore volume (V_{micro}), mesopore volume (V_{meso}), and pore size distribution, PSD, of ACC were yielded by using the software of the apparatus. PSD was determined using both BJH and DFT methods as will be mentioned later in Section 3.1.

The pH_{pzc} value of washed ACC which is the pH of the solution when the net charge on ACC piece dipped into it is zero, was determined in our previous work [18] using batch equilibrium method described by Babič et al. [19].

2.4. Adsorption cell

A specially designed cell was used to carry out the adsorption studies and simultaneously to perform in situ concentration measurements by means of UV absorption spectrophotometry. This cell, described in detail including a diagram in our previous works [12,14], was V-shaped with one arm containing ACC attached to a short Pt wire sealed to a glass rod and the other arm containing a thin glass tube through which N_2 gas was passed for the purposes of mixing and eliminating any dissolved CO_2. The two arms were connected to a glass joint leading to a vacuum pump at the upper part of the V-shaped cell in order to provide the opportunity for initial outgassing of the carbon adsorbent. A quartz spectrophotometer cuvette was sealed to the bottom of the adsorption cell.

2.5. Optical absorbance measurements

A Varian cary 100 model UV/vis spectrophotometer was used for optical absorbance measurements. The absorbance measurements were conducted in situ for the study of the kinetics of adsorption process. In all experiments, the size and mass of ACC was kept as constant as possible (about 28.0 ± 0.1 mg). Weighed ACC pieces were pre-wetted by leaving in water for

24 h before use. The idea of using pre-wetted ACC originates from previous findings that pre-wetting enhances the adsorption process [12,13].

A pre-wetted ACC piece was dipped into the adsorption cell initially containing only water and vacuum was applied to remove all air in the pores of ACC. Then wetted and degassed ACC piece was removed from the cell for a short time and water in the cell was replaced with a known volume of sample solution (20 ml). The sliding door of the sample compartment of the spectrophotometer was left half-open and the quartz cuvette fixed at the bottom of the adsorption cell (which now contained the sample solution) was inserted into the front sample compartment. A teflon tube connected to the tip of a thin N_2-bubbling glass tube was lowered from one arm of the adsorption cell down the UV cell to a level just above the light path to provide effective mixing. Finally, the ACC piece which was removed temporarily after wetting and degassing was inserted from the other arm of the adsorption cell into the solution. Then, quickly, an opaque curtain was spread above the sample compartment of the spectrophotometer, over the cell, to prevent interference from external light. The temperature of the adsorbate solution was kept constant at $25 \pm 1\,^{\circ}C$ during the adsorption process using a termostated cell holder in the sample compartment of the spectrophotometer.

The program for monitoring the absorbance at a specific wavelength of maximum absorbance pre-determined by taking the whole spectrum of each dye was then run on the software of the spectrophotometer. Absorbance data were recorded in programmed time intervals of 1 min until the equilibrium is reached.

Absorbance data were converted into concentration data using calibration relations pre-determined at the wavelength of interest for each dye.

2.6. Determination of adsorption isotherms

The adsorption isotherms of acid dyes onto ACC were determined on the basis of batch analysis. ACC pieces of varying weights were allowed to equilibrate with dye solutions of constant initial concentration at 25 °C for 48 h. The initial concentration was 3.0×10^{-5} M for AB45, AB92, AB120 and 4.0×10^{-5} M for AB129. Preliminary tests showed that the concentration of dye solutions remained unchanged after 8–21 h contact with ACC depending on the type of dye. So, the allowed contact time of 48 h ensures the equilibration for all four dyes. The equilibrium concentrations of dye solutions were measured spectrophotometrically. The amount of dyes adsorbed per unit mass of ACC at equilibrium, q_e, was calculated by Eq. (1):

$$q_e = \frac{V(c_0 - c_e)}{m} \quad (1)$$

where V is the volume of dye solution in liters, c_0 and c_e are the initial and equilibrium concentrations, respectively, of the dye solutions in mol L^{-1} and m is the mass of ACC in grams. Eq. (1) gives q_e as mol dye adsorbed per grams of ACC.

3. Results and discussion

3.1. Characteristics of ACC

The specific surface area of ACC (S_{BET}) was calculated according to Brunauer, Emmet, Teller method [20] using the linear part of the nitrogen adsorption isotherm shown in Fig. 2. S_{BET} was determined as 1870 $m^2\,g^{-1}$. The total volume of pores, V_{tot}, was calculated as 0.827 $cm^3\,g^{-1}$ using the volume value at the relative pressure of 0.995 from Fig. 2. The pore size distribution (PSD) for mesopores and micropores were calculated using BJH (Barrett, Joyner, Halenda) and DFT (density functional theory) methods [21,22] respectively, and the resulting distribution curves are given in Figs. 3 and 4. Total mesopore volume (V_{meso}) was determined as 0.082 $cm^3\,g^{-1}$ and total micropore volume (V_{micro}) was determined as 0.709 $cm^3\,g^{-1}$ from the corresponding methods. The ACC consists of pores mainly in micro character (<20 Å) as seen both from Figs. 3 and 4. The pH_{pzc} value of ACC used in this study had been previously found to be 7.4 [18].

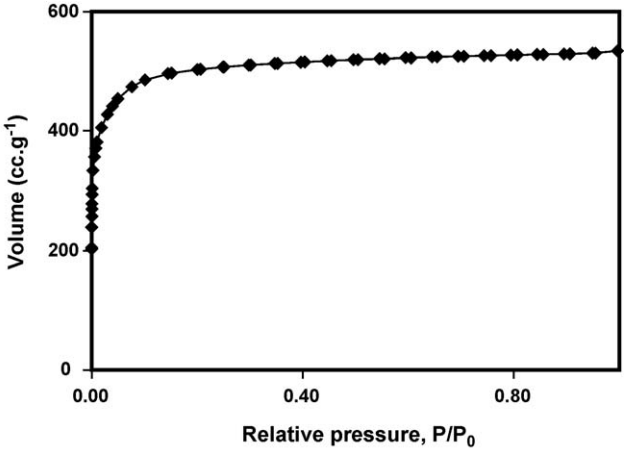

Fig. 2. Nitrogen adsorption isotherm at 77.4 K for ACC studied.

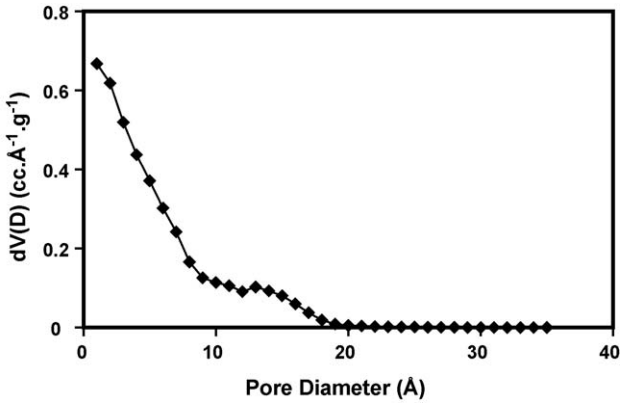

Fig. 3. Pore size distribution of ACC according to BJH theory.

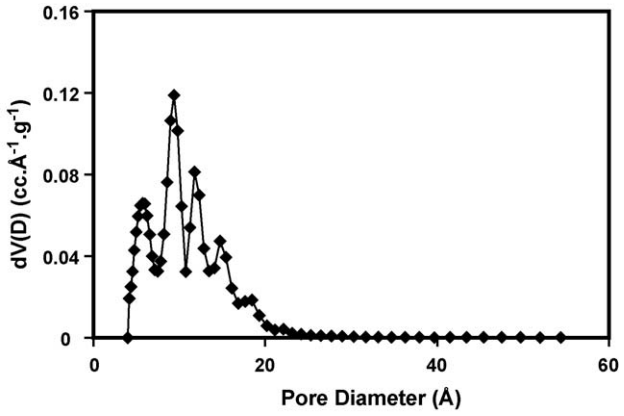

Fig. 4. Pore size distribution of ACC according to DFT theory.

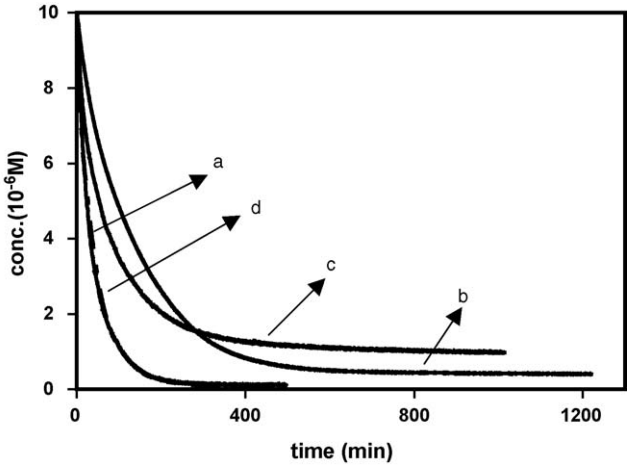

Fig. 5. Adsorption behaviors of acid dyes; a: AB45, b: AB92, c: AB120 and d: AB129 from aqueous solutions onto ACC.

3.2. Absorption characteristics of dyes

Absorption properties and calibration data for the four dyes studied are given in Table 1. In order to obtain the calibration curve of each dye, absorbances were measured at the corresponding λ_{max} as a function of concentration and the data were fitted to Lambert–Beer Law by the method of least square analysis. The resulting regression coefficients (r) given in the last column of Table 1 show that the fit to Lambert–Beer law is excellent. These calibration curves were used to convert absorbance data into concentrations in kinetic and equilibrium studies of adsorption of dyes.

3.3. Adsorption kinetics of dyes

Adsorption of dyes onto ACC was monitored spectrophotometrically by the procedure described above. Absorbance data, obtained in 1-min intervals until equilibrium, were converted into concentration data using the corresponding calibration relations and then plotted as a function of time in Fig. 5 for each dye. Adsorption equilibrium times, determined as the time after which the concentration of the dye solution remained unchanged during the course of adsorption process, were 445, 1225, 1020 and 498 min for AB45, AB92, AB120 and AB129, respectively. In order to compare adsorption behaviors of dyes, the initial concentrations (1.0×10^{-5} M) and volumes (20 mL) of dye solutions and the mass of ACC (28.0 ± 0.1 mg) were taken to be the same for the adsorption study of each dye. As seen in Fig. 5, concentration versus time curves of AB45 and AB129 almost overlap. At the early stages of adsorption AB120 seems to be adsorbed faster than AB92 but in the later stages the opposite is observed as indicated by the crossover of their corresponding curves in Fig. 5. Concentrations of dyes AB45, AB92, AB120 and AB129 in solution decreased to 4.6×10^{-8}, 4.0×10^{-7}, 9.7×10^{-7} and 1.1×10^{-7} M, respectively, all from the same initial concentration of 1.0×10^{-5} M, by adsorption onto ACC until their equilibrium times. In other words, concentrations of dyes in aqueous solution were reduced by a factor of approximately 217 for AB45, 25 for AB92, 10 for AB120 and 91 for AB129 over the course of adsorption.

Table 1
Spectrophotometric and calibration parameters for the dyes

Dyes	λ_{max} (nm)	ε (a.u. cm^{-1} M^{-1})	r
AB45	241	80900	0.9999
AB92	218	105000	0.9998
AB120	274	32500	0.9991
AB129	628	17900	1.0000

Three kinetic models were applied to adsorption kinetic data in order to investigate the behavior of adsorption process of dyes onto ACC. These models are the pseudo-first-order [23], the pseudo-second-order [24] and the intraparticle diffusion models [15]. Linear form of pseudo-first-order model can be formulated as

$$\ln(q_e - q_t) = \ln(q_e) - k_1 t \quad (2)$$

where q_e (mol g^{-1}) and q_t (mol g^{-1}) are the amount of dye adsorbed at equilibrium and at time t, respectively, and k_1 (min^{-1}) is the rate constant. k_1 values were evaluated from the linear regression of $\ln(q_e - q_t)$ versus t data for each dye and are tabulated in Table 2. In this Table the experimental q_e values calculated using initial and equilibrium concentrations (Fig. 5) of each dye according to Eq. (1) and q_e values from the intercept of linear regression analysis according to the model (Eq. (2)) are also given.

The linear form of pseudo-second-order equation can be formulated as

$$\frac{1}{q_t} = \frac{1}{k_2 {q_e}^2} + \frac{1}{q_e} t \quad (3)$$

where k_2 (g mol^{-1} min^{-1}) is the second-order rate constant. The linear plot of t/q_t as a function of t provided not only the rate constant k_2, but also an independent evaluation of q_e. The results are given in Table 2. The fit of experimental data to the pseudo-first-order and the pseudo-second-order equations seemed to be quite good when correlation coefficients (r) obtained from linear regression analysis were examined (r values are not given but all are greater than 0.9). However, it is very difficult to decide

Table 2
Calculated and experimental q_e values and the first-order and the second-order rate constants

Dyes	q_e (mol g^{-1}) (experimental)	First-order			Second-order		
		k_1 (min^{-1})	P	q_e (mol g^{-1}) (calculated)	k_2 (g mol^{-1} min^{-1})	P	q_e (mol g^{-1}) (calculated)
AB45	7.11×10^{-6}	3.13×10^{-3}	17.17	4.40×10^{-6}	6147.44	4.10	7.55×10^{-6}
AB92	6.86×10^{-6}	5.53×10^{-3}	25.23	3.51×10^{-6}	1863.05	4.82	7.39×10^{-6}
AB120	6.45×10^{-6}	5.30×10^{-3}	11.12	2.52×10^{-6}	4104.33	1.68	6.71×10^{-6}
AB129	7.07×10^{-6}	1.32×10^{-2}	84.11	2.44×10^{-6}	6959.53	5.41	7.43×10^{-6}

which model represents the experimental data best just on the basis of regression coefficients. A better criterion to find the best model for the experimental data is a parameter known as normalized percent deviation [25] or in some literature percent relative deviation modulus, P, [26] defined by the following equation

$$P = \left(\frac{100}{N}\right) \sum \left(\frac{|q_t(\text{expt}) - q_t(\text{pred})|}{q_t(\text{expt})} \right) \quad (4)$$

where $q_{t(expt)}$ is the experimental q_t at any t, $q_{t(pred)}$ is the corresponding predicted q_t according to the equation under study with best fitted parameters, N is the number of data points. It is clear that the lower the P value, the better is the fit. When the P values given in Table 2 are examined, it can be seen that they are much smaller for the second-order model than for the first-order model leading to a conclusion that the kinetic data of adsorption of dyes onto ACC fit to the second-order model better than the first-order model. Furthermore, the experimental and calculated q_e values are in good agreement with each other according to the second-order model (Table 2). The second-order rate constants of dyes are found to decrease in the following order; AB129 > AB45 > AB120 > AB92. The kinetics of adsorption of many dye species onto various adsorbent was also found to be of second-order in literature; adsorption of Direct Blue 2B and Direct Green B on sawdust based activated carbon [27], adsorption of Congo Red on bagasse fly ash, on commercial and laboratory grade activated carbon [28], and on coir pith [29], adsorption of Direct Red 23 and Direct Red 80 on orange peel [30], adsorption of Basic Blue 9 on pyrophyllite [31], on Fe(II)/Cr(III) hydroxide [32] and on cyclodextrin based material [33], and adsorption of Reactive Blue 2, Reactive Red 2, Reactive Yellow 2, Reactive Yellow 86, Acid Orange 12, Acid Red 14, Acid Orange 7 and Acid Red 81 on cross-linked chitosan [34].

Kinetic data of adsorption of dyes were also tested according to intraparticle diffusion model which can be formulated as

$$q_t = k_i t^{1/2} + I \quad (5)$$

where k_i (mol g^{-1} min$^{-1/2}$) is the intraparticle diffusion rate constant and I (mol g^{-1}) is a constant. The fit of experimental data to q_t versus $t^{1/2}$ line predicted by Eq. (5) was poor with P values much higher than those given in Table 2 for the first-order and the second-order models. Thus the possibility of this model to be applicable to the adsorption kinetics of the dyes studied was eliminated.

3.4. Adsorption isotherms

Adsorption isotherms of dyes were determined on the basis of batch analysis at 25 °C using a series of dye solutions at fixed concentration and volume in contact with ACC pieces of varying masses. Adsorption isotherm data of dyes were fitted to well-known and widely applied isotherm models of Langmuir and Freundlich. The Langmuir isotherm is based on the assumption that adsorption takes place at specific homogeneous sites within the adsorbent and there is no significant interaction among adsorbed species and that the adsorbent is saturated after one layer of adsorbate molecules formed on the adsorbent surface. The linearized Langmuir isotherm equation can be written as follows

$$\frac{c_e}{q_e} = \frac{1}{bq_m} + \frac{c_e}{q_m} \quad (6)$$

where q_e (mol g^{-1}) is the amount of solute adsorbed per unit mass of adsorbent, c_e (mol L^{-1}) is the equilibrium concentration of solute, q_m (mol g^{-1}) is the maximum amount of adsorbate to form a complete monolayer on the surface, b (L mol^{-1}) is a constant related to the heat of adsorption. When c_e/q_e is plotted against c_e and the data are regressed linearly, q_m and b constants can be calculated from the slope and the intercept.

The Freundlich isotherm model takes the multilayer and heterogeneous adsorption into account. Its linearized form can be given as follows:

$$\ln q_e = \ln K + \frac{1}{n} \ln c_e \quad (7)$$

where q_e and c_e have the same definitions as in Langmuir equation above. Freundlich constant, K (mol$^{1-(1/n)}$ L$^{1/n}$ g^{-1}) is related to the adsorption capacity of ACC and $1/n$ is another constant related to the surface heterogeneity. When $\ln q_e$ is plotted against $\ln c_e$ and the data are treated by linear regression analysis, $1/n$ and K constants are determined from the slope and intercept. The value of $1/n$ is known as the heterogeneity factor and ranges between 0 and 1; the more heterogeneous the surface, the closer $1/n$ value is to 0 [35].

The Langmuir and Freundlich isotherm parameters for the adsorption of dyes studied onto ACC are given in Table 3. Experimental isotherm data for the four dyes are given in Figs. 6–9 where the fitted Langmuir and Freundlich isotherm curves are also shown. As in the case of examining the goodness of fit of kinetic models to experimental data, the regression coefficients alone were insufficient in determining the best isotherm model to

Table 3
The parameters of Langmuir and Freundlich isotherm equations for the adsorption of dyes

Dyes	Langmuir			Freundlich		
	q_m (mol g^{-1})	b (L mol^{-1})	P	K (mol$^{1-(1/n)}$ L$^{1/n}$ g^{-1})	$1/n$	P
AB45	1.38×10^{-4}	646	13.91	4.85×10^{-3}	0.322	2.99
AB92	7.12×10^{-5}	584	2.10	6.75×10^{-4}	0.212	4.00
AB120	4.03×10^{-5}	556	3.51	3.66×10^{-4}	0.193	3.59
AB129	1.34×10^{-4}	431	10.76	1.92×10^{-3}	0.256	2.65

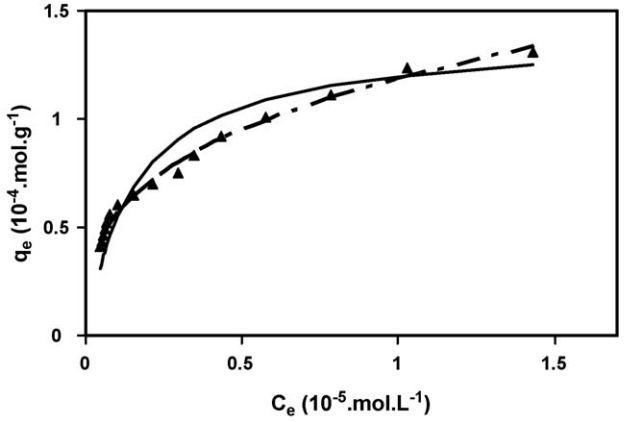

Fig. 6. The fit of experimental adsorption data (▲) to Langmuir (—) and Freundlich (- - -) models for AB45.

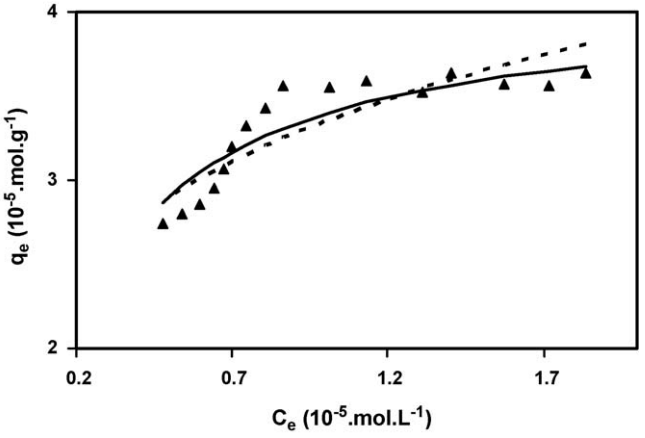

Fig. 8. The fit of experimental adsorption data (▲) to Langmuir (—) and Freundlich (- - -) models for AB120.

represent the experimental data because they were mostly greater than 0.9 for both models. So, again a P parameter defined by an equation similar to Eq. (4) with q_t terms replaced by q_e terms was used as a criterion in finding the best isotherm model to fit the experimental data. These P values are included in Table 3. In general, it is accepted that when the P value is less than 5, the fit of data to the model is considered to be excellent. The P values for Freundlich model are much less than 5 for all four dyes. So, it can be concluded that Freundlich model is good for representing the adsorption isotherm data of the dyes studied. However it is also seen that Langmuir model is almost equally good for AB92 and AB120. Adsorption capacities for the dyes determined by q_m parameter of Langmuir model or K parameter of Freundlich model follow the same order; AB45 > AB129 > AB92 > AB120.

This order can be correlated with the sizes of dye molecules as well as the pore size distribution of ACC used. Visually, it is obvious from the molecular structures given in Fig. 1 that the sizes of AB92 and AB120 are significantly larger than those of AB45 and AB129. Unfortunately, the exact sizes of all dye molecules are not available. Only the size of AB45 is given as 3.8 Å in radius and 13 Å in length by Han et al. [36]. The pore size distribution of ACC used in the present work given in Fig. 4 shows that this dye molecule, considering its length, fits only to slightly less than half of the micropores available. Considering the increasing number of additional aromatic rings in the order AB45 < AB129 < AB92 < AB120, one can estimate the sizes of these dye molecules to increase in the same order.

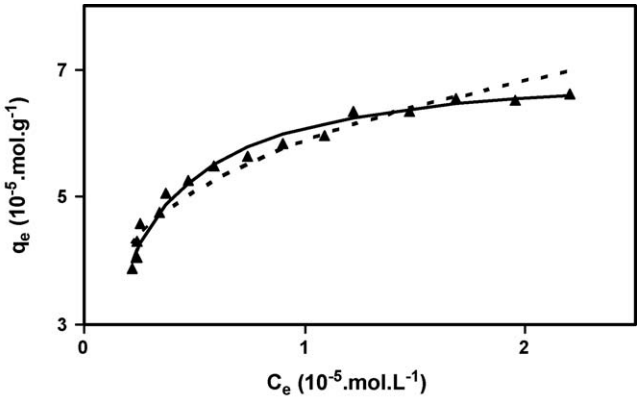

Fig. 7. The fit of experimental adsorption data (▲) to Langmuir (—) and Freundlich (- - -) models for AB92.

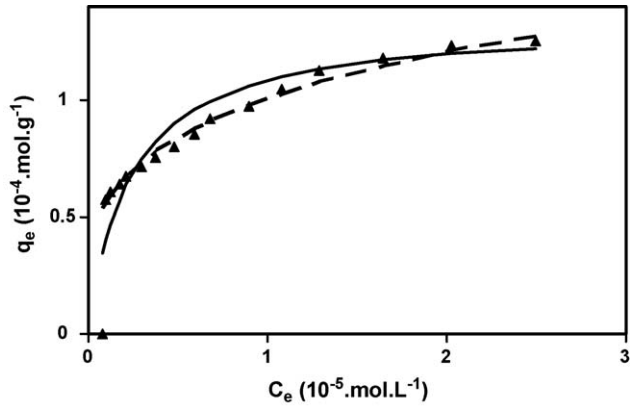

Fig. 9. The fit of experimental adsorption data (▲) to Langmuir (—) and Freundlich (- - -) models for AB129.

Since the smallest one just fits to half of the micropores, others are expected to fit to smaller portions of micropores. It should also be recognized that molecules may also penetrate to the pores from their smaller sides, 7.6 Å in the case of AB45. However, it is clear, in general, that there is a close correlation between the sizes of dye molecules and the pore sizes of ACC.

3.5. *pH–pH_{pzc} relation and types of interactions involved in adsorption*

The pH values of dye solutions with an initial common concentration of 1.0×10^{-5} M were measured as 6.63, 5.68, 5.34 and 5.83 at the beginning of adsorption and as 6.60, 6.46, 6.60 and 6.37 at equilibrium for AB45, AB92, AB120 and AB129, respectively. It can be seen that pH values of all dye solutions are close to each other and the change in pH during the whole course of adsorption is not too much, the largest change being 1.26 pH unit for AB120. These results indicate that pH of dye solutions is not a determining factor for the trend observed in kinetic and equilibrium data for the adsorption of dyes. On the other hand, the measured pH values are slightly smaller than the pH_{pzc} value (7.4) of ACC. This suggests that the surface of ACC in these dye solutions has a small net positive charge as they all have pH values smaller than 7.4. Since all dye species carry some negative charge due at least to sulfonate groups (Fig. 1), electrostatic attractions are expected to have a considerable contribution to the overall interactions. Furthermore, dispersive interactions and some hydrogen bonding interactions should still be operative between dye species and ACC surface.

4. Conclusion

It was found that the dyes AB45, AB92, AB120 and AB129 can be removed to a great extent from aqueous solutions by adsorption onto ACC. Adsorption of these dyes was found to follow second-order kinetic model with the following order of rate constants AB129 > AB45 > AB120 > AB92. The order of adsorption capacities for the dyes according to both Langmuir and Freundlich isotherm models was found to be as follows AB45 > AB129 > AB92 > AB120 and this order was found to be correlated with the sizes of dyes and pore size distribution of ACC.

Acknowledgements

Authors thank to the Scientific Research Projects Unit of Akdeniz University for the support of this work through the project 2003.01.0300.009, to the Spectra Corp. (MA, USA) for providing the ACC and to METU for carrying out measurements to determine the surface properties of the ACC.

References

[1] M.A. Al-Ghouti, M.A.M. Khraisheh, S.J. Allen, M.N. Ahmad, The removal of dyes from textile wastewater: a study of the physical characteristics and adsorption mechanisms of diatomaceous earth, J. Environ. Manage. 69 (2003) 229–238.

[2] G. McKay, M.S. Otterburn, D.A. Aga, Fuller's earth and fired clay as adsorbent for dye stuffs. Equilibrium and rate constants, Water Air Soil Poll. 24 (1985) 307–322.

[3] K.K.H. Choy, J.F. Porter, G. McKay, Intraparticle diffusion in single and multicomponent acid dye adsorption from wastewater onto carbon, Chem. Eng. J. 103 (2004) 133–145.

[4] A. Dabrowski, Adsorption—from theory to practice, Adv. Colloid Interface 93 (2001) 135–224.

[5] T. Robinson, G. McMullan, R. Marchant, P. Nigam, Remediation of dyes in textile effluents; a critical review on current treatment technologies with a proposed alternative, Bioresource Technol. 77 (2001) 247–255.

[6] J.-M. Chern, J.-Y. Wu, Desorption of dye from activated carbon beds: effects of temperature, pH, and alcohol, Water Res. 35 (2001) 355–368.

[7] K. Kadirvelu, C. Karthika, N. Vennilamani, S. Pattabhi, Activated carbon from industrial solid waste as an adsorbent for the removal of Rhodamine-B from aqueous solution: kinetic and equilibrium studies, Chemosphere 60 (2005) 1009–1017.

[8] X. Yang, B. Al-Duri, Kinetic modeling of liquid-phase adsorption of reactive dyes on activated carbon, J. Colloid Interface Sci. 287 (2005) 25–34.

[9] M.K. Purkait, S. DasGupta, S. De, Adsorption of eosin dye on activated carbon and its surfactant based desorption, J. Environ. Manage. 76 (2005) 135–142.

[10] F. Banata, N. Al-Bastakib, Treating dye wastewater by an integrated process of adsorption using activated carbon and ultrafiltration, Desalination 170 (2004) 69–75.

[11] C. Brasquet, P. Le Cloirec, Adsorption onto activated carbon fibers: application to water and air treatments, Carbon 35 (1997) 1307–1313.

[12] E. Ayranci, B.E. Conway, Adsorption and electrosorption at high-area carbon felt electrodes for waste-water purification: systems evaluation with inorganic, S-containing anion, J. Appl. Electrochem. 31 (2001) 257–266.

[13] E. Ayranci, B.E. Conway, Adsorption and electrosorption of ethyl xanthate and thiocyanate anions at high-area carbon-cloth electrodes studied by in situ UV spectroscopy: development of procedures for wastewater purification, Anal. Chem. 73 (2001) 1181–1189.

[14] E. Ayranci, N. Hoda, Studies on removal of metribuzin, bromacil, 2,4-D and atrazine from water by adsorption on high area carbon cloth, J. Hazard. Mater. B 112 (2004) 163–168.

[15] E. Ayranci, N. Hoda, Adsorption kinetics and isotherms of pesticides onto activated carbon-cloth, Chemosphere 60 (2005) 1600–1607.

[16] C. Brasquet, P. Le Cloirec, Adsorption onto activated carbon fibers: application to water and air treatments, Carbon 35 (1997) 1307–1313.

[17] C. Faur-Brasquet, K. Kadirvelu, P. Le Cloirec, Removal of metal ions from aqueous solution by adsorption onto activated carbon cloths: adsorption competition with organic matter, Carbon 40 (2002) 2387–2392.

[18] O. Duman, E. Ayranci, Structural and ionization effects on the adsorption behaviors of some anilinic compounds from aqueous solutions onto high area carbon-cloth, J. Hazard. Mater. B120 (2005) 173–181.

[19] B.M. Babić, S.K. Milonjić, M.J. Polovina, B.V. Kaludierović, Point of zero charge and intrinsic equilibrium constants of activated carbon cloth, Carbon 37 (1999) 477–481.

[20] S. Brauner, P.H. Emmet, E. Teller, Adsorption of gases in multimolecular layers, J. Am. Chem. Soc. 60 (1938) 309–319.

[21] E.P. Barrett, L.G. Joyner, P.P. Halenda, The determination of pore volume and area distribution in porous substances. I. Computations from nitrogen isotherms, J. Am. Soc. 73 (1951) 373–380.

[22] N.A. Seaton, J.P.R.B. Walton, N. Quirke, New analysis method for the determination of the pore size distribution of porous carbons from nitrogen adsorption measurements, Carbon 27 (6) (1989) 853–861.

[23] S. Lagergren, About the theory of so-called adsorption of soluble substances, Kungliga Svenska Vetenskapsakademiens, Handlinger 24 (4) (1898) 1–39.

[24] G. McKay, Y.S. Ho, Pseudo-second order model for sorption process, Process. Biochem. 34 (1999) 441–465.

[25] R.-S. Juang, R.-L. Tseng, F.-C. Wu, S.-H. Lee, Liquid-phase adsorption of phenol and its derivatives on activated carbon fibers, Sep. Sci. Technol. 31 (1996) 1915–1931.
[26] E. Ayranci, A.C. Dalgic, Moisture sorption isotherms of pistacia terebinthus L. and its protein isolate, Lebensm-Wiss. Technol. 25 (1992) 482–483.
[27] P.K. Malik, Dye removal from wastewater using activated carbon developed from sawdust: adsorption equilibrium and kinetics, J. Hazard. Mater. B113 (2004) 81–88.
[28] I.D. Mall, V.C. Srivastava, N.K. Agarwal, I.M. Mishra, Removal of congo red from aqueous solution by bagasse fly ash and activated carbon: kinetic study and equilibrium isotherm analyses, Chemosphere 61 (2005) 492–501.
[29] C. Namasivayam, D. Kavitha, Removal of Congo Red from water by adsorption onto activated carbon prepared from coir pith, an agricultural solid waste, Dyes Pigments 54 (2002) 47–58.
[30] M. Arami, N.Y. Limaee, N.M. Mahmoodi, N.S. Tabrizi, Removal of dyes from colored textile wastewater by orange peel adsorbent: equilibrium and kinetic studies, J. Colloid Interf. Sci. 288 (2005) 371–376.
[31] A. Gücek, S. Şener, S. Bilgen, M.A. Mazmancı, Adsorption and kinetic studies of cationic and anionic dyes on pyrophyllite from aqueous solution, J. Colloid Interf. Sci. 286 (2005) 53–60.
[32] C. Namasivayam, S. Sumithra, Removal of direct red 12B and methylene blue from water by adsorption onto Fe(III)/Cr(III) hydroxide, an industrial solid waste, J. Environ. Manage. 74 (2005) 207–215.
[33] G. Crini, H.N. Peindy, Adsorption of C.I. Basic Blue 9 on cyclodextrin-based material containing carboxylic groups, Dyes Pigments 70 (2006) 204–211.
[34] M.-S. Chiou, P.-Y. Ho, H.-Y. Li, Adsorption of anionic dyes in acid solutions using chemically cross-linked chitosan beads, Dyes Pigments 60 (2004) 69–84.
[35] B. Al Duri, Adsorption modeling and mass transfer, in: G. McKay (Ed.), Use of adsorbents for the removal of pollutants from wastewaters, CRC Press Inc, Florida, 1995, pp. 133–173.
[36] S. Han, K. Sohn, T. Hyeon, Fabrication of new nanoporous carbons through silica templates and their application to the adsorption of bulky dyes, Chem. Mater. 12 (2000) 3337–3341.